Numerical Investigation of Flow Effects on Accuracy in Turbine Flow Meters

Th. Hüwener, E. von Lavante*, Reinhard Ernst**, W. M. Schieber****

*University of Essen, Essen, Germany

** Ruhrgas AG, Dorsten, Germany

*** American Meter Company, Erie, Pa, USA

Abstract: The present paper describes 2-D numerical simulations of a new class of turbine flow meters with two counterrotating rotors. The main goal was to investigate stator/rotor interactions and to improve the accuracy of the meter. The impact of stator/rotor interaction on the variation of coefficient of tangential force is shown. An improved design with a modified guide vane is proposed. Experimental results of the accuracy curves for the original and the modified guide vane are shown.

Keywords: Turbine Flow Meter, Accuracy, Stator/Rotor Interaction, Self-Proving

1 Introduction and Theory of Operation

Due to the extensive industrial and home use of natural gas, a widespread transportation system of gas pipelines operating at high pressures has been developed. At present, the majority of flow metering needed to effectively operate this system is being done by using turbine flowmeters or orifice plates. Baker [1] gives a good overview of the theoretical and experimental published information in the field of turbine flow metering.

In the past two decades research was done on self-correcting and self-checking turbine flow meters. One working principle is based on the coupling of two rotors. A sensor rotor small distance downstream from the main rotor senses and responds to changes in the exit angle of the fluid leaving the main rotor [2, 3].

Another working principle assumes two decoupled rotors, where the second, the so-called reference rotor, works independent of the first stage. The resulting two-stage turbine meter, capable of evaluating its own accuracy under actual operating flow rates and pressures without interrupting the normal service of the meter, has been investigated in the last years [4, 5].

Figure 1 shows a cutaway drawing of the AccuTest^{TM} two-stage turbine flow meter.

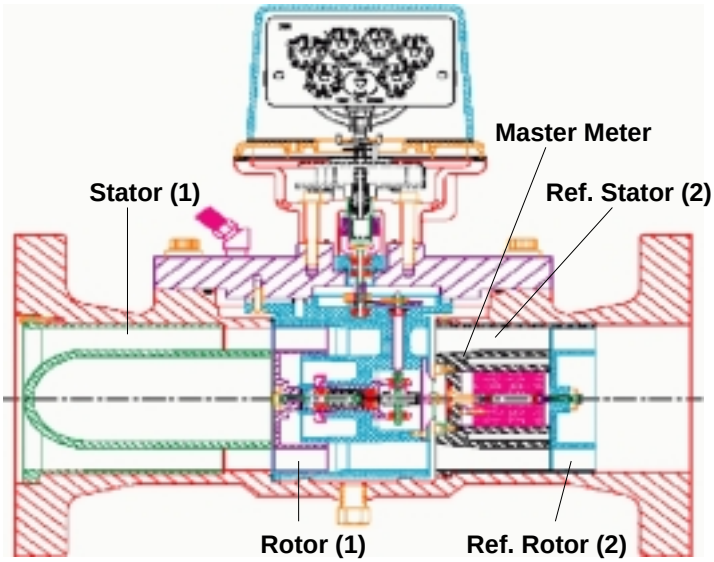

Figure 1. Cutaway drawing of the two-stage AccuTest^{TM} turbine flow meter.

The design of the flow meter consists of two parts. The front part, with the gas entering from the left, is a slight modification of an existing, conventional meter. The second part is a so-called

master meter, designed to achieve the self-proving feature of the meter. It is a separate free-running turbine meter cartridge. Rotor speed is measured with an electronic sensor that detects the rotor blade tips as they pass the proximity of the sensor. The function of the master meter is to evaluate the accuracy of the main meter.

For steady flow, the accuracy is defined as

$$Acc = \frac{\dot{Q}_{meter}}{\dot{Q}_{std}} \tag{1}$$

where $\dot{Q}_{meter}$ is the volume flow rate measured in the meter and $\dot{Q}_{std}$ is the flow rate measured by a proving standard. $\dot{Q}_{std}$ is assumed to be 100% accurate. The k factor is defined as the ratio of the total number of output pulses to the actual volume of gas that passed through the meter. When considering the same time periods, $k = f/\dot{Q}$ becomes the ratio of the output frequency over the actual flowrate. The k factor is by definition 100% accurate. The rotor speed is uniquely related to the flow rate since the gear ratio in the meter remains always the same. Assuming that the meter operates mostly at its half capacity, the k factor taken as a reference value corresponds to this flowrate. This k factor is the nominal factor k_{nom}. It is:

$$k = k_{nom} \cdot Acc_{lab} \tag{2}$$

where Acc_{lab} is the accuracy at a particular flow rate and pressure obtained during initial calibration of the meter. The flow rate measured by the mechanical output is

$$\dot{Q}_{meter} = \frac{f}{k_{nom}} \tag{3}$$

Then, substituting Eq. (3) into Eq. (1), gives

$$Acc = \frac{\frac{f}{k_{nom}}}{\dot{Q}_{std}} \tag{4}$$

Now the accuracy of the reference rotor by definition is assumed to be one, resulting in

$$Acc_{SPM} = \frac{Acc_{main}}{Acc_{ref}} = Acc_{main} \tag{5}$$

where the subscript SPM denotes the self-proving meter. Substituting Eq. (4) in Eq. (5) yields:

$$Acc_{SPM} = \frac{\frac{f_{main}}{k_{nom,main}}}{\frac{f_{ref}}{k_{ref}}} \tag{6}$$

Finally, substituting Eq. (2) into Eq. (6) yields

$$Acc_{SPM} = \frac{f_{main}}{f_{ref}} \cdot \frac{k_{ref}}{k_{main}} \cdot Acc_{lab}. \tag{7}$$

This is the resulting working relationship, which is true as long as the master meter remains 100% accurate.

One major benefit of the two-stage turbine meter over a conventional turbine meter is a reduced need of inspection and maintenance, requiring only one person with a laptop or a so-called electronic flow computer. Furthermore, the meter performance is monitored for immediate detection of accuracy changes and the effects of flow disturbances. Installation effects as velocity profile deformation and swirl are weaker due to an improved guide vane design of the first stage [4].

However, in order to optimize the design and accuracy of the two-stage turbine meter even further, the flow field inside the meter has to be analyzed. Since it is rather difficult to investigate the flow in the meter experimentally, it was decided to simulate the flow numerically. The details of the numerical simulation of the turbine meter are explained below.

2 Numerical Simulation

A 2-D cascade model (Figure 2), located at the mean-radius between rotor hub and tip was set up with $22,000$ grid points. In the present simulations, an undisturbed velocity profile was used initially at the inlet of the first stage of the meter in order to reduce the numerical grid to the size of one rotor/stator blade in each stage of the turbine meter. The boundaries between the blades could therefore be treated as periodic.

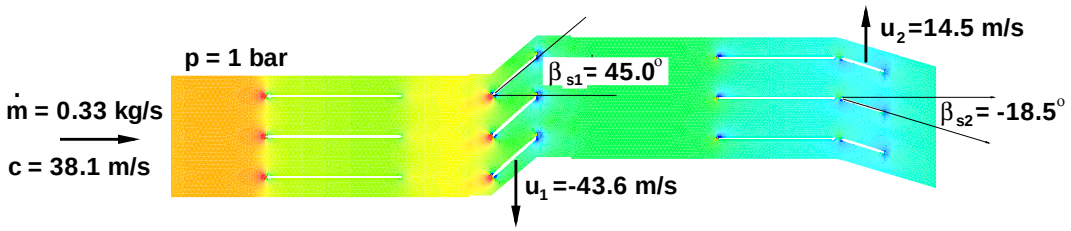

Figure 2. Flow Conditions and Geometry of the numerical simulation.

The simulations were performed using a time dependent coupled explicit solver, using a 2-nd order implicit unsteady method in pseudo-time. The second order upwind discretization scheme was chosen to achieve acceptable accuracy. The k-epsilon turbulence model with its standard model constants was judged to be adequate. Even if the occuring incoming Mach numbers are smaller than 0.16, the flow is assumed to be compressible because Mach numbers up to 0.3 appear when the flow is accelerated around the trailing edge. Therefore, ideal gas law was used.

Initially, the time step size in the numerical simulations was $\Delta t = 10\ ms$, corresponding to 60 time steps one rotor blade of the first stage needs to pass one stator blade section. After a time periodic fluctuation of mass flow rate in certain axial planes, and coefficient of tangential blade force was reached, the times step size was increased by a factor of 3. Pressure inlet and outlet conditions were used to yield the desired mass flow rates. This procedure requires adjusting the outlet pressure to a proper value in several iteration steps, and is very time consuming.

The numerical simulations were performed with air at a gas pressure of $1\ bar$, a total temperature $T_0 = 293.15\ K$ and mass flow rate of $0.33\ kg/s$, corresponding to a Mach number of $Ma = 0.11$ in the blade sections of the turbine meter. The speed of rotation of both rotors was adjusted by approximately $2\ \%$ to yield a ratio of rotor speeds of $u_1/u_2 = 3/1$. This assures periodic flow conditions every three periods of the first stage, corresponding to one period of the second stage. The values are $u_1 = -42.71\ m/s$ and $u_2 = 14.24\ m/s$.

One of the special design features of the current design is a so-called trailing edge flap, implemented in order to improve the meter accuracy at small flow rates. Its function will be discussed in the following chapter. Due to the very small gap between the second stator and rotor, the stator/rotor interactions were analyzed im more detail.

3 Results

The simulated pressure drop obtained in the turbine flow meter was $\Delta p = 1260\ Pa$, which satisfies the requirements of permissible pressure drop, published in the DIN-Norm 33800 [6].

Based on the analysis of the trailing edge flap and the stator/rotor interactions a modified guide vane design in the second stage is tested numerically. Finally experimental results focusing on accuracy curves for the original and modified guide vane design are presented.

3.1 Trailing Edge Flap

A well known problem in turbine flow metering is the reduced accuracy for small volumetric flow rates $\dot{Q}$. In order to improve the meters' behaviour at small flow rates, it is necessary to produce a sufficient lift force in rotational direction of the rotor blades even for small volumetric flow rates. This can be done by increasing the angle of incidence; however, excessive angles of incidence lead to nonlinearities in the flow field. Therefore, a modification to the rotors was added to increase the camber of the rotors. The modification consists of a trailing edge flap, similar to an airplane wing in landing configuration, shown in detail in Figure 3.

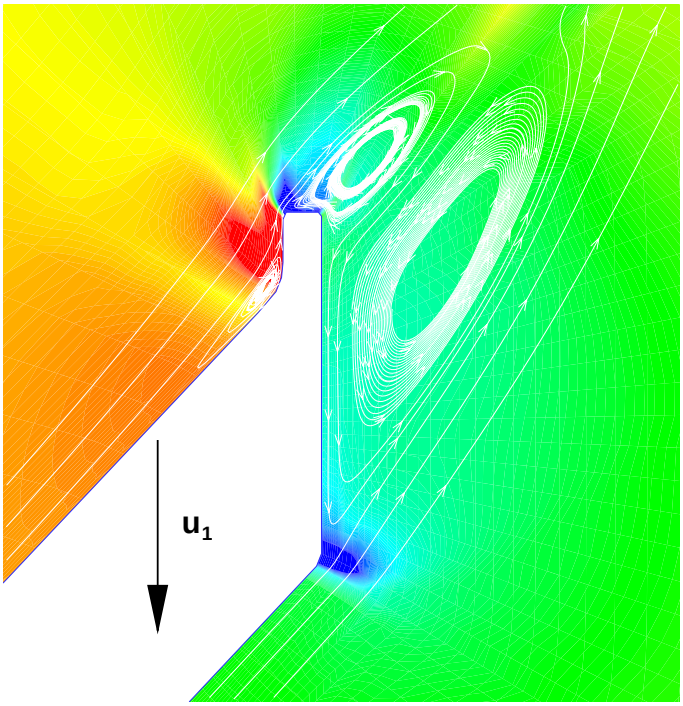

Figure 3. Pressure contours and streamlines of relative velocity at the trailing edge of the first rotor.

On the pressure side of the rotor, a stagnation point develops, yielding high pressure values. In the wake behind the trailing edge, a low pressure region originates. The streamlines visualize two counterrotating vortices. The one on top of the flap, originates at the front side of the trailing edge flap. Here, backflow can be seen on top of the trailing edge flap. The other vortex in the wake of the rotor originates at the bottom side of the trailing edge flap. Detailed analysis of the flow around the trailing edge flap showed that the vorticity significantly depends on the incoming Mach number.

3.2 Stator/Rotor Interactions

The numerical simulations focused on the stator/rotor interactions, especially in the second stage, because the axial gap between second stator and second rotor is very small. The following Figure 4 shows the density contours in the second stage for one period and 6 time steps.

It can be seen at every time that the non-aerodynamically formed trailing edge of the reference rotor produces a large wake region of low density. In the wake, the entropy reaches very large values. While the reference rotor passes the reference stator($t = 0$, $t = 1/6\ T_2$), unfavourable flow effects occur. These stator/rotor interactions result in low densities on the pressure side of the reference rotor, while the rotor passes the wake of the stator. This low density region is convected from the

leading edge of the pressure side of the rotor($t = 1/6\ T_2$) along the pressure side until it is dissipated at $t = 3/6\ T_2$. At $t = 3/6\ T_2$ and $t = 4/6\ T_2$, the rotor is completly outside the stator wake and no significant density variations on the rotor blade occur.

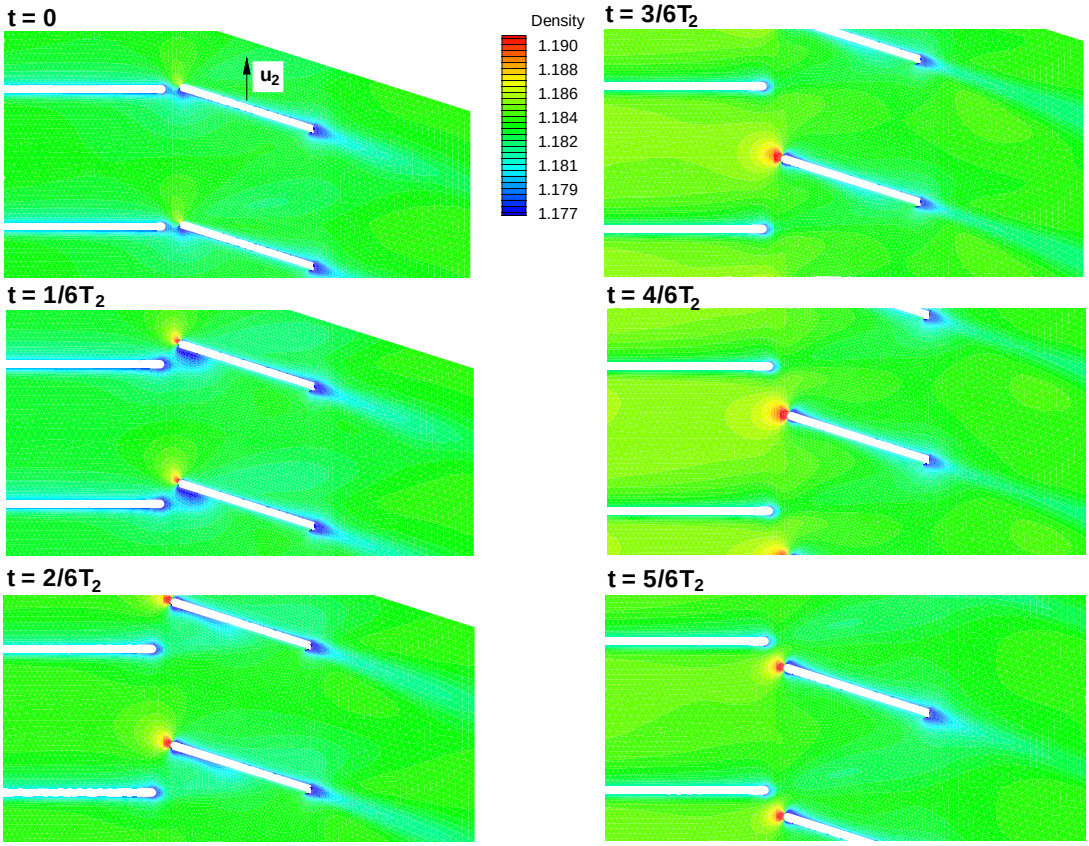

Figure 4. Density contours for one period of the second stage of the turbine flow meter.

A time dependent analysis of the coefficient of tangential force, defined as

$$c_t = \frac{T}{\frac{1}{2}\rho_{ref} \cdot w_{ref}^2 \cdot l_{ref} \cdot b}, \tag{8}$$

is used to show the stator/rotor interactions quantitatively. Here, T is the tangential force acting on each blade, the subscript ref denotes a reference state that is given by the inlet conditions, w is the relative incoming flow velocity, l_{ref} the chord length and b a fictive height of the blade. The following Figure 5 shows the coefficient of tangential force c_t of both stators and rotors versus time after a periodic state is reached.

As expected, the coefficient of tangential force of the first stator is zero because of the undisturbed inlet flow conditions and an angle of incidence of zero degrees. The coefficient of tangential force of the first rotor is negative with an averaged coefficient of tangential force of $c_t = -0.16$ and an amplitude of 0.08. The frequency of the coefficient of tangential force of the first rotor corresponds to the time T_1, the first rotor needs to pass one stator section.
The coefficient of tangential force of the reference stator (2) is $c_t = 0.19$ with an amplitude of 0.05 caused by the disturbed flow conditions from the outlet of the first stage. Because of the strong stator/rotor interactions in the master meter, the amplitude of the coefficient of tangential force of the reference rotor (2) is 0.31 with an averaged value of $c_t = -0.03$. Here, the frequency of the coefficient of tangential force corresponds to the time T_2 the reference rotor (2) needs to pass one stator section.

Additional plots of the mass flow rate versus time for the inlet and outlet planes of both stages

show a high variation of the flow rate at both outlet planes, caused by the wakes of the rotors.

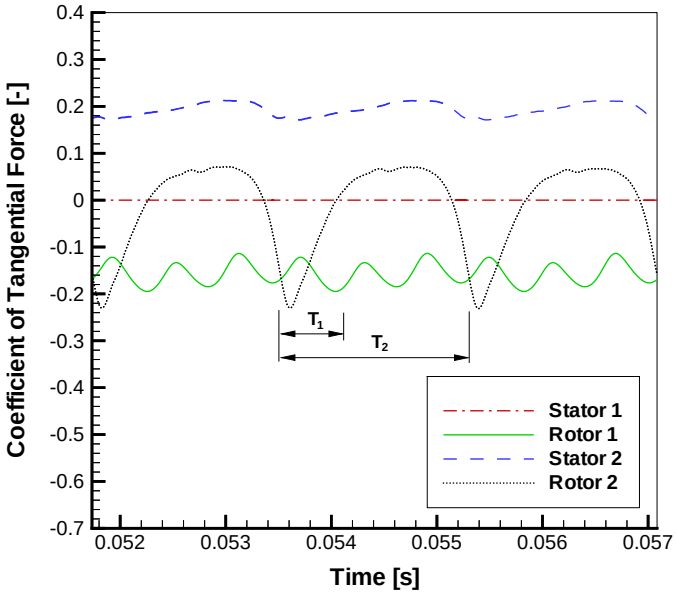

Figure 5. Coefficient of tangential force versus time for both stators and rotors for a periodic state.

In a first step of optimization of the design of the turbine flow meter, the variation of coefficient of tangential force and mass flow rate in the master meter should be improved. From the flow field and additional pressure plots on the top and bottom side of the reference stator it was seen that no flow conditioning occured in the last third of the stator. Thus a design with a shortened second stator was implemented to improve the effects of stator/rotor interaction and to minimize the variation of the coefficient of tangential force in the reference rotor.

Figure 6 shows a comparison of the coefficient of tangential force of the reference stator (2) and the reference rotor (2) for the original design and the design with the shortened reference stator.

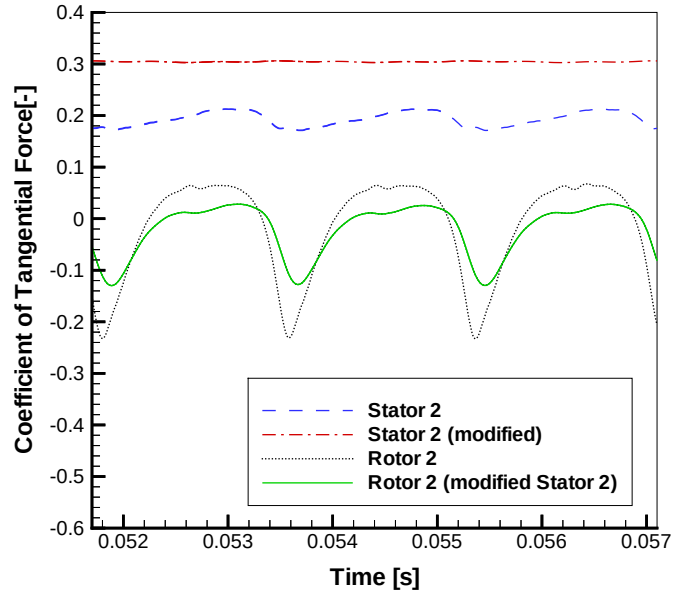

Figure 6. Comparison of coefficient of tangential force of reference stator (2) and reference rotor (2) for the original and the modified design with a shortened reference stator (2).

The plots show a rotor coefficient of tangential force that was reduced about 47% in amplitude in comparison to the original design. This implies that the influence of the reference stator's wake on the rotor was decreased dramatically.
Furthermore, an increased value of the coefficient of tangential force of the reference guide vane can be seen. The reason is the shortened reference length l_{ref} in the calculation of the coefficient of tangential force; the absolute force T on the stator remains the same as in the original design. This proves that no flow conditioning occured at the back part of the stator in the original design. In the new design, the amplitude was reduced to approximately zero. The reason for this change is the increased distance to the second rotor and the reduced amplitude of mass flow rates.
Additional evaluation of the mass flow rate showed that the amplitude in the exit plane of the master meter is reduced by 45% with the usage of the modified shortened reference guide vane.

3.3 Experiments

After the numerical simulations showed good results for the design with the shortened reference stator (2), experiments were made to study the influence of the modifications on the rotor's accuracy curve. These tests were performed at AMCO's test facility in Erie at operating pressures of $27\ psi$ and $100\ psi$. Figure 7 shows the accuracy curves of both rotors for the old and new design at a pressure of $27\ psi$.

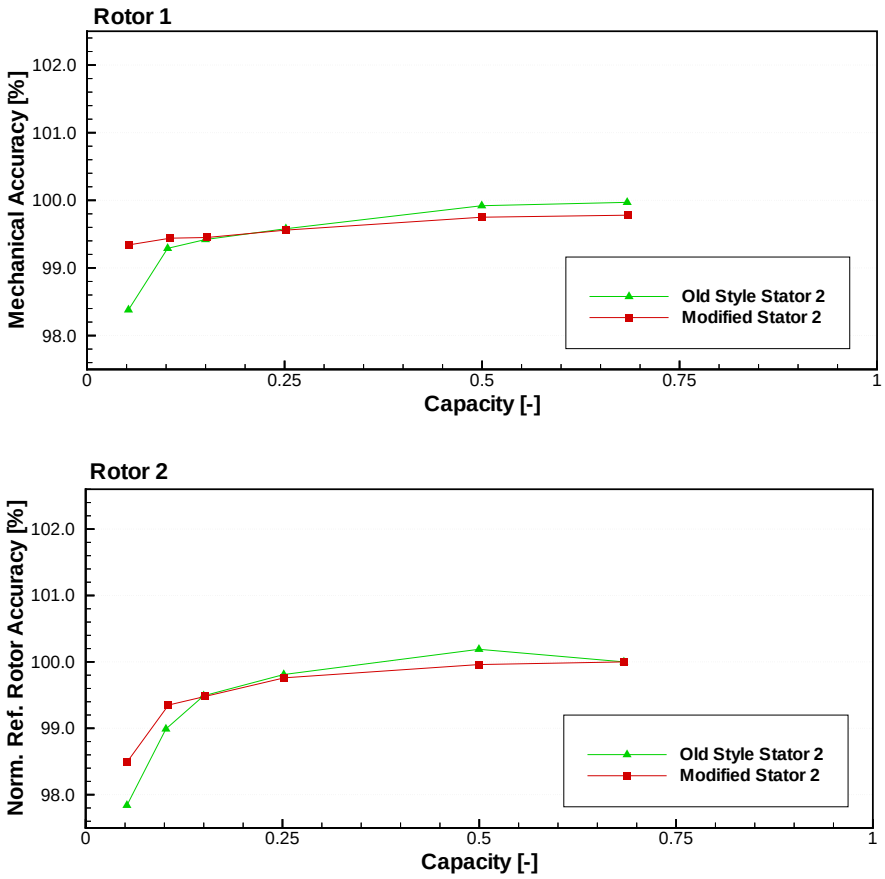

Figure 7. Comparison of accuracy curves for the original and the modified design of the second stator at a pressure of $27\ psi$.

The accuracy curve of rotor 1 shows an improved linearity over the whole range of the volumetric flowrate $\dot{Q}$ in comparison with the accuracy curve for the original design. Especially for small flow rates the modified design shows an improved accuracy. Comparsion of the accuracy curves of the second rotor reveals also an improved linearity in the whole flow range and a positive shift in accuracy for small flow rates. However, the improvement in the accuracy curve of the second rotor is less significant than in the case of the first rotor.

3 Conclusions

The present numerical simulations help to understand the flow inside the turbine flow meter, for instance the function of the trailing edge flap can be explained in detail. The analysis of the time dependent coefficients of tangential force c_t implied that the design of the master meter, especially the distance between stator and rotor, could be improved. Initial calculations showed that the amplitude of the mass flow rate in the exit plane as well as the coefficient of tangential force of the reference rotor could be reduced by more than 45% by shortening the length of the reference guide vane. These numerically results were confirmed by experiments showing an improved linearity of the accuracy curves and a positive shift in the accuracy curve for small flow rates.

References

[1] R. C. Baker. Turbine Flowmeters: II. Theoretical and Experimental published Information. *Flow Measurement and Instrumentation*, 4(3):123–144, 1993.

[2] D. J. Gestler. The Auto-Adjust Turbo-Meter and how it Developed. *Pipeline & Gas Journal*, July, 1980.

[3] W. F. Z. Lee, D. C. Blakeslee, and R. V. White. A Self-Correcting and Self-Cecking Gas Turbine Meter. *Journal of Fluids Engineering*, 104:143–149, 1982.

[4] W. Schieber. A Turbine Meter with Built-in Transfer Prover. In *Proceedings of the 9th International Conference on Flow Measurement, FLOMEKO '98*, pages 509–516, Lund, Sweden, June, 15-17, 1998.

[5] W. Schieber. *United States Patent, No. 5,866,824*. American Meter Company, 1999.

[6] *Turbinenradgaszähler, DIN Norm 33800*. Berlin, 1986.

AUTHOR(S):

Dipl. Ing. Thomas Hüwener, Prof. Dr.-Ing. Ernst von Lavante, Institute of Turbomachinery, University of Essen, D-45127 Essen, Germany, phone +49 (0)201-183-2901,
E-mail: thomas@tigger.turbo.uni-essen.de, erni@tigger.turbo.uni-essen.de;
Dipl. Ing. R. Ernst, Ruhrgas AG, Halterner Str. 125, D-46284 Dorsten, phone +49 (0)2362-93-8593,
E-mail: reinhard.ernst@ruhrgas.com; Germany;
W. M. Schieber, American Meter Company, 920 Payne Avenue, Erie, Pa 16512, USA,
Email: schieb2@aol.com